

Journal Pre-proof

Indazolyl-substituted piperidin-4-yl-aminopyrimidines as HIV-1 NNRTIs: Design, synthesis and biological activities

Ting Xiao, Jia-Fan Tang, Ge Meng, Christophe Pannecouque, Yuan-Yuan Zhu, Gen-Yan Liu, Zhi-Qiang Xu, Feng-Shou Wu, Shuang-Xi Gu, Fen-Er Chen



PII: S0223-5234(19)31016-5

DOI: <https://doi.org/10.1016/j.ejmech.2019.111864>

Reference: EJMECH 111864

To appear in: *European Journal of Medicinal Chemistry*

Received Date: 4 October 2019

Revised Date: 25 October 2019

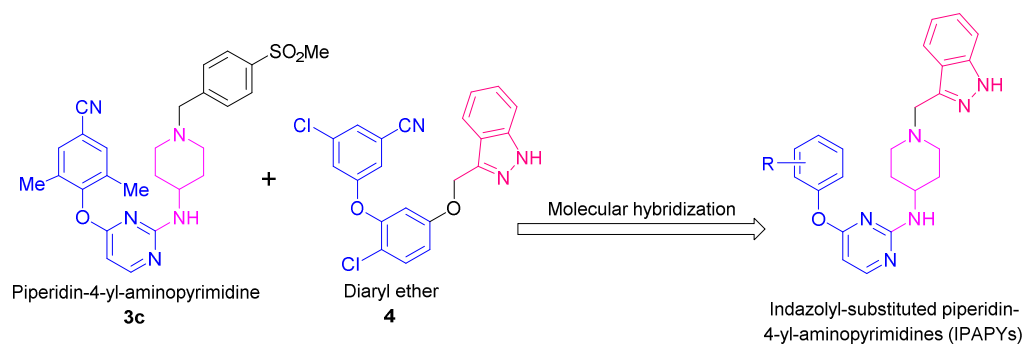
Accepted Date: 6 November 2019

Please cite this article as: T. Xiao, J.-F. Tang, G. Meng, C. Pannecouque, Y.-Y. Zhu, G.-Y. Liu, Z.-Q. Xu, F.-S. Wu, S.-X. Gu, F.-E. Chen, Indazolyl-substituted piperidin-4-yl-aminopyrimidines as HIV-1 NNRTIs: Design, synthesis and biological activities, *European Journal of Medicinal Chemistry* (2019), doi: <https://doi.org/10.1016/j.ejmech.2019.111864>.

This is a PDF file of an article that has undergone enhancements after acceptance, such as the addition of a cover page and metadata, and formatting for readability, but it is not yet the definitive version of record. This version will undergo additional copyediting, typesetting and review before it is published in its final form, but we are providing this version to give early visibility of the article. Please note that, during the production process, errors may be discovered which could affect the content, and all legal disclaimers that apply to the journal pertain.

© 2019 Published by Elsevier Masson SAS.

Graphical abstract



15n, R=2,6-diMe, EC_{50} (WT HIV-1) =8.6 nM, SI=2093;
15q, R=2,6-diMe-4-CN, EC_{50} (WT HIV-1) =6.4 nM, SI=2500.

Indazolyl-substituted piperidin-4-yl-aminopyrimidines as

HIV-1 NNRTIs: design, synthesis and biological activities

Ting Xiao^{a, 1}, Jia-Fan Tang^{a, 1}, Ge Meng^b, Christophe Pannecouque^c, Yuan-Yuan Zhu^d,
Gen-Yan Liu^a, Zhi-Qiang Xu^a, Feng-Shou Wu^a, Shuang-Xi Gu^{a, *}, Fen-Er Chen^{a, b, *}

^a Key Laboratory for Green Chemical Process of Ministry of Education, School of Chemical Engineering & Pharmacy, Wuhan Institute of Technology, Wuhan 430205, China

^b Department of Chemistry, Fudan University, Shanghai 200433, China

^c KU Leuven, Department of Microbiology and Immunology, Laboratory of Virology and Chemotherapy, Rega Institute for Medical Research, B-3000 Leuven, Belgium

^d School of Chemistry and Environmental Engineering, Wuhan Institute of Technology, Wuhan 430205, China

¹ Authors Ting Xiao and Jia-Fan Tang contributed equally to this work.

* Corresponding authors

E-mail addresses: shuangxigu@163.com (S.-X. Gu), rfchen@fudan.edu.cn (F.-E. Chen)

Abstract: A series of indazolyl-substituted piperidin-4-yl-aminopyrimidines (IPAPYs) were designed from two potent HIV-1 NNRTIs piperidin-4-yl-aminopyrimidine **3c** and diaryl ether **4** as the lead compounds by molecular hybridization strategy. The target molecules **5a-q** were synthesized and evaluated for their anti-HIV activities and cytotoxicities in MT-4 cells. **5a-q** displayed moderate to excellent activities against wild-type (WT) HIV-1 with EC₅₀ values ranging from 1.5 to 0.0064 μM. Among them, **5q** was regarded as the most excellent compound against WT HIV-1 (EC₅₀ = 6.4 nM, SI = 2500). And also, it displayed potent activities against K103N (EC₅₀ = 0.077 μM), Y181C (EC₅₀ = 0.11 μM), E138K (EC₅₀ = 0.057 μM), and moderate activity against double mutants RES056 (EC₅₀ = 8.7 μM). Moreover, the structure-activity relationships (SARs) were summarized, and the molecular docking was performed to investigate the binding mode of IPAPYs and HIV-1 reverse transcriptase.

Keywords: AIDS; Anti-HIV; NNRTIs; Piperidin-4-yl-aminopyrimidines; Molecular hybridization

1. Introduction

Reverse transcriptase (RT) plays a vital role in the process of the human immunodeficiency virus type 1 (HIV-1) replication [1,2]. Nonnucleoside reverse transcriptase inhibitors (NNRTIs), known as one of the indispensable components of highly active antiretroviral therapy (HAART) for specifically inhibiting HIV-1, have received wide attention due to their potent antiviral activity, high specificity and low cytotoxicity [3-5]. In the past decades, many series of NNRTIs have sprung up to fight against HIV-1/AIDS [6], such as benzophenones [7,8], dihydroalkoxybenzyl-oxypyrimidines (DABOs) [9,10], diaryl ethers [11,12], diaryltriazines (DATAs) [13,14], and diarylpyrimidines (DAPYs) [15,16] and so on. Among them, diarylpyrimidines (DAPYs, Fig. 1), represented by FDA-approved drugs etravirine (TMC125, Fig. 1) and rilpivirine (TMC278, Fig. 1), have been recognized as one of the most successful classes of NNRTIs developed so far due to their excellent potency against wild-type (WT) HIV-1 and its mutant strains. In recent years, a great deal of DAPYs and their analogues emerged as HIV-1 NNRTIs [17-21].

In earlier years, the 4-cyanophenylamino structure (wing I) was regarded as the essential pharmacophore of classical DAPYs (Fig. 1). However, in 2010, Tang & Kertesz group [22,23] combined the structure of DAPYs and the benzophenones to design piperidin-4-yl-aminopyrimidines **3a-c** (Fig. 1), which showed potent activities against WT HIV-1 (7-34 nM) as well as HIV-1 mutants. It demonstrated that phenyl- or benzyl-substituted piperidine was also an excellent pharmacophore which could replace the 4-cyanophenylamino (wing I) of classical DAPYs. More importantly, it is well-known that the pharmacokinetic profiles of most DAPYs are not satisfactory due to low water solubility, while piperidine-linked aminopyrimidine derivatives could improve the water solubility and bioavailability [24,25]. Based on these, medicinal chemists have discovered dozens of new series of piperidin-4-yl-aminopyrimidines as HIV-1 NNRTIs [15,25,26].

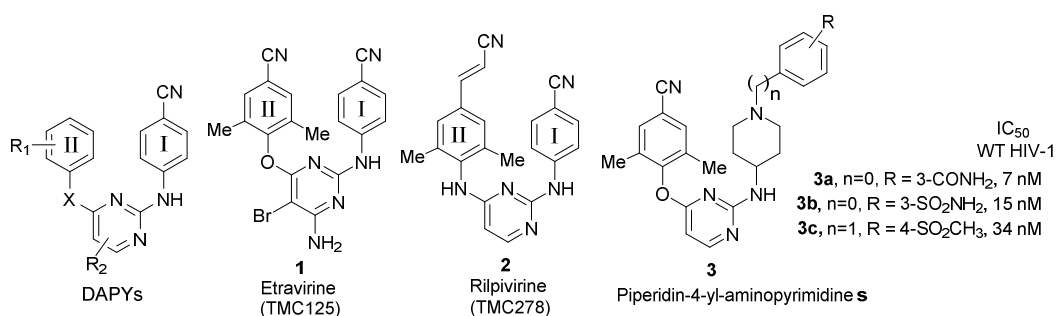
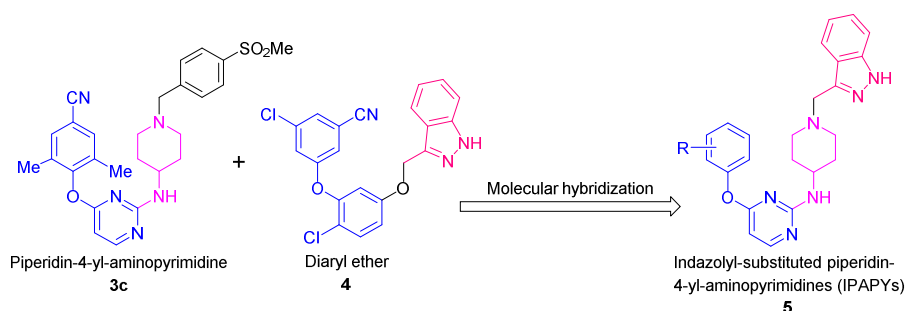


Fig. 1 Structures of classical DAPYs and their analogues

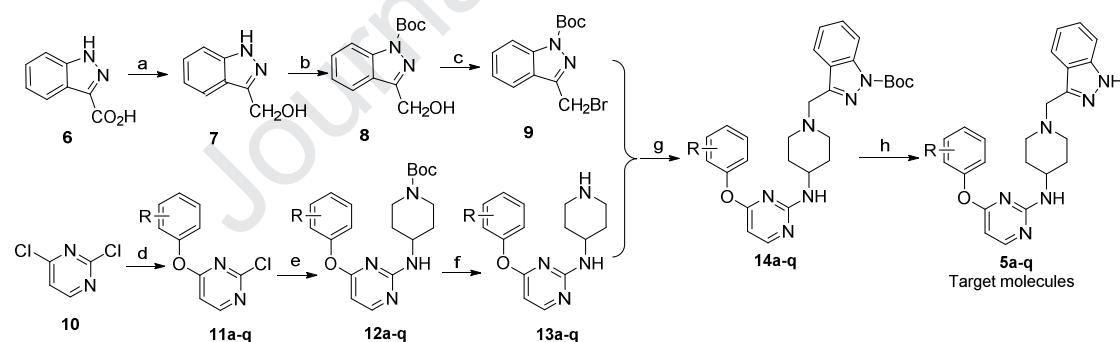
Herein, the structures of piperidin-4-yl-aminopyrimidine **3c** [22] and diaryl ether **4** [27] as two potent HIV-1 NNRTIs, were hybridized to design a novel series of indazolyl-substituted piperidin-4-yl-aminopyrimidines (**5**, IPAPYs, Fig. 2), which were synthesized and evaluated for their anti-HIV activities as well as their cytotoxicities. Their structure-activity relationships were summarized, and the molecular docking was performed to investigate their binding mode.

Fig. 2 Design of target molecules **5** by molecular hybridization

2. Results and discussion

2.1 Chemistry

The synthetic route of the target compounds **5a-q** is shown in Scheme 1. The key intermediate 1-Boc-3-bromomethylindazole **9** was synthesized from 1*H*-indazole-3-carboxylic acid **6** as a starting material via three-step reactions including reduction, NH protection and bromination, successively. Meanwhile, the key intermediates **13a-q** were prepared from 2,4-dichloropyrimidine **10** by two nucleophilic reactions followed by removal of the protecting group Boc. Then, **14a-q** were obtained by a nucleophilic substitution reaction of **9** and **13a-q** using K_2CO_3 as base in the presence of 18-crown-6 in THF. Finally, the intermediates **14a-q** were subjected to deprotection of amino group to get the corresponding target compounds **5a-q**.



Compd	R	Compd	R	Compd	R
5a	2-Cl	5g	2-CF ₃	5m	4-CN
5b	3-Cl	5h	3-CF ₃	5n	2,6-diMe
5c	4-Cl	5i	4-CF ₃	5o	3-Cl-5-CN
5d	2-Br	5j	3-CH ₃	5p	3,5-diMe-4-Cl
5e	3-Br	5k	4-CH ₃	5q	2,6-diMe-4-CN
5f	4-Br	5l	3-CN		

Scheme 1. Reagents and conditions: (a) $LiAlH_4$, THF; (b) Boc_2O , dimethylaminopyridine, triethylamine, THF; (c) PBr_3 , DMF; (d) substituted phenol, *N,N*-diisopropylethylamine, DMSO; (e) 4-amino-1-Boc-piperidine, *N,N*-diisopropylethylamine, NMP; (f) CF_3COOH , DCM, rt; (g) K_2CO_3 ,

18-crown-6, THF; (h) CF₃COOH, DCM, rt.

2.2 Biological activity

The 3-(4,5-dimethylthiazol-2-yl)-2,5-diphenyl-tetrazolium bromide (MTT) method [28,29] was used to evaluate 17 new IPAPYs (**5a-q**) along with five FDA-approved drugs: zidovudine, lamivudine, nevirapine, etravirine, efavirenz as reference drugs. The compounds were assayed for their anti-HIV activities in MT-4 cells against WT HIV-1 (strain IIIB), common HIV-1 mutants [K103N, Y181C, E138K, K103N+Y181C (RES056)], as well as HIV-2 (strain ROD). The results were summarized in Table 1, which were expressed as CC₅₀ (50% cytotoxic concentration), EC₅₀ (50% HIV-1 replication inhibitory concentration) as well as SI (selectivity index given by the CC₅₀/EC₅₀ (IIIB) ratio) values.

As shown in Table 1, compounds **5a-q** displayed moderate to excellent activities against WT HIV-1 with EC₅₀ values ranging from 1.5 to 0.0064 μM. Among them, the two most potent compounds **5n** and **5q** displayed extremely potent WT HIV-1 inhibitory activities with EC₅₀ values of 8.6 nM and 6.4 nM, respectively, which surpassed the corresponding activities of the FDA-approved zidovudine, lamivudine and nevirapine.

The 17 target molecules are chemically and biologically diverse. Among the compounds **5a-f**, the two molecules **5a** (EC₅₀ = 0.037 μM) and **5d** (EC₅₀ = 0.031 μM) with an ortho substituent were obviously superior to **5b-c** and **5e-f** (EC₅₀ = 0.21-0.28 μM) with a meta- or para-substituent in WT inhibitory activities. The replacement of the halogen atoms of **5a-f** with a trifluoromethyl (**5g-i**) led to a dramatic decrease of activities. For compounds **5a-i** bearing a halogen atom or CF₃, the substituent priority is as follows, -Br ≥ -Cl > -CF₃.

For compounds **5j-k** bearing an electron-donating methyl group, the para-methyl (**5k**, EC₅₀ = 0.14 μM) seemed to be more favorable than meta-methyl (**5j**, EC₅₀ = 0.39 μM). For compounds **5l-m** bearing an electron-withdrawing cyano group, the para-CN (**5m**, EC₅₀ = 0.078 μM) showed an overwhelming priority for anti-HIV-1 IIIB activity compared with meta-CN (**5l**, EC₅₀ = 1.5 μM). Not surprisingly, the compound **5q**, featuring a 2,6-diMe-4-CN-Ph left wing which was the same as the left wing of etravirine (Fig. 1), displayed the most potent activities against WT HIV-1 (EC₅₀ = 6.4 nM). While 4-CN of **5q** was removed, the corresponding compound **5n** also exhibited excellent activity against WT HIV-1 (EC₅₀ = 8.6 nM). The two compounds **5o** (EC₅₀ = 2.3 μM) and **5p** (EC₅₀ = 0.37 μM) with 3- and 5-substituents were inferior to the two compounds **5n** (EC₅₀ = 0.086 μM) and **5q** (EC₅₀ = 0.064 μM) with a 2,6-dimethyl.

All target molecules have also been evaluated for their activities against the RT mutants (K103N, Y181C, E138K, RES056). Most of compounds **5a-q** showed moderate activities against single mutants K103N, Y181C and E138K, and were nearly devoid of activities against double mutants RES056 as well as HIV-2 (ROD). The most excellent compound **5q** displayed potent activities against K103N (EC₅₀ = 0.077 μM), Y181C (EC₅₀ = 0.11 μM), E138K (EC₅₀ = 0.057 μM), and moderate activity against RES056 (EC₅₀ = 8.7 μM).

Table 1 Anti-HIV activities and cytotoxicities of **5a–q** in MT-4 cells.^a

Compd	EC ₅₀ ^b (μM)					ROD ^c (μM)	CC ₅₀ ^d (μM)	SI ^e
	III _B	K103N	Y181C	E138K	RES056			
5a	0.037	>5.4	1.6	0.80	>5.4	>5.4	5.4	146
5b	0.28	9.8	9.0	4.7	>26	>26	26	93
5c	0.23	4.0	5.6	2.3	>30	>30	30	130
5d	0.031	1.9	1.0	0.48	>5.3	>5.3	5.3	171
5e	0.25	4.9	6.1	3.5	>22	>22	22	88
5f	0.21	5.7	7.5	2.0	>24	>24	24	114
5g	0.30	8.3	6.8	4.4	>15	>15	15	50
5h	0.55	8.9	9.7	7.0	>22	>22	22	40
5i	0.47	10	>29	4.8	>29	>29	29	62
5j	0.39	9.6	≥11	4.0	>32	>32	32	82
5k	0.14	3.8	4.3	0.77	>32	>32	32	229
5l	1.5	>32	>32	>32	>32	>32	32	21
5m	0.078	2.6	3.13	1.4	>31	>31	31	397
5n	0.0086	0.22	0.40	0.084	>18	>18	18	2093
5o	2.3	>27	>27	>27	>27	>27	27	12
5p	0.37	8.2	8.7	4.7	>15	>15	15	41
5q	0.0064	0.077	0.11	0.057	8.7	>16	16	2500
Zidovudine	0.018	0.019	0.012	0.019	0.028	0.021	>7.5	>417
Lamivudine	3.10	2.0	2.4	2.9	5.0	NA	>87	>28
Nevirapine	0.15	5.6	10	0.16	>15	>15	>15	>100
Etravirine	0.0032	0.0032	0.014	0.0067	0.034	NA	>4.6	>1438
Efavirenz	0.0026	0.076	0.0050	0.0044	0.24	NA	>6.3	>2423

^a Data represent the mean of at least three independent experiments.

^b Compound concentration required to protect MT-4 cells against HIV-1-induced cytopathogenicity by 50%.

^c Compound concentration required to protect MT-4 cells against HIV-2-induced cytopathogenicity by 50%.

^d Compound concentration that decreases the uninfected MT-4 cell viability by 50%.

^e Selectivity index: CC₅₀/EC₅₀ (III_B) ratio.

2.3 Molecular modeling analysis

To investigate the binding mode of our newly synthesized compounds, the molecular docking studies of the two representative compounds **5n** and **5q** were performed by using the SYBYL Surflex-Dock program and crystal structure of WT HIV-1 RT/**3c** (PDB code: 3NBP) [30]. As illustrated in Fig. 3, compounds **5q** (Fig. 3a) and **5n** (Fig. 3b) displayed similar binding mode as **3c** in NNIBS, adopting similar “U” shape binding mode. π - π stacking interaction formed between the left wing of compounds **5n** (or **5q**) and the aromatic amino acid residues Tyr181, Tyr188 and Trp229. And a key hydrogen bond formed between the hydrogen of NH liner and the carbonyl of

Lys101. Moreover, the piperidinyl-linked indazole moiety extended to the protein-solvent interface, and another hydrogen-bonding interaction was found to form between the NH of the indazole and the main chain of Lys103. For another, as illustrated in Fig. 3, the binding mode of the left wing of **5n** and **5q** showed almost perfect coincidence. And the 2,6-dimethyl-4-cyano fragment of **5q** could build extensive interactions with sub pocket composed by hydrophobic amino acid residue Trp229, Thr181 and Phe227.

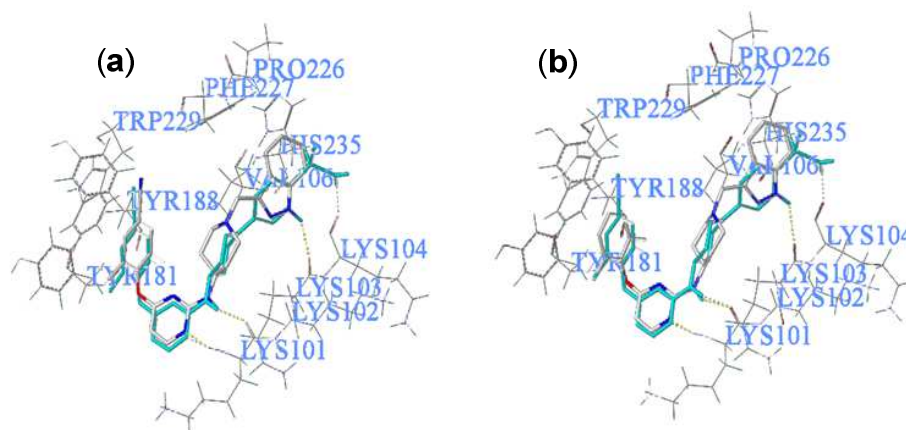


Fig. 3. a) Binding mode of **5q** (gray) and overlap with **3c** (cyan) in NNIBS; b) Binding mode of **5n** (gray) and overlap with **3c** (cyan) in NNIBS.

3. Conclusion

In summary, as a continuing effort to develop novel NNRTIs, a series of structurally diverse analogues of indazolyl-substituted piperidin-4-yl-aminopyrimidines (IPAPYs) were designed and synthesized. The results of biological activities indicated that all target compounds showed good to excellent activities against WT HIV-1 strain. Among them, **5q** was regarded as the most excellent compound against WT HIV-1 ($EC_{50} = 6.4$ nM, SI = 2500). And also, it displayed potent activities against K103N ($EC_{50} = 0.077$ μ M), Y181C ($EC_{50} = 0.11$ μ M), E138K ($EC_{50} = 0.057$ μ M), and moderate activity against RES056 ($EC_{50} = 8.7$ μ M). The preliminary structure-activity relationships were summarized, and the molecular docking was performed to investigate the binding mode of representative inhibitors and HIV-1 RT, which laid a foundation for the further development of new DAPY analogues as NNRTIs.

4. Experimental

4.1. Chemistry

Melting points were measured on a SGW X-4B microscopic melting-point apparatus. Nuclear magnetic resonance (NMR) spectra on two Varian spectrometers (400, 600, 800 MHz for 1 H NMR; 200 MHz for 13 C NMR) were recorded in DMSO- d_6 or $CDCl_3$. Chemical shifts were reported in δ (ppm) units relative to the internal standard tetramethylsilane. For most of target

molecules, high resolution mass spectra (HRMS) was obtained on an Agilent Q-TOF6300 instrument, and the deviation between the calculated values and measured values of HRMS is less than 5%. And for others, mass spectra was obtained on a Waters Quattro Micromass instrument using electrospray ionization (ESI) techniques. All chemicals and solvents were of reagent grade and purified and dried by standard methods before use. All the reactions were monitored by thin layer chromatography (TLC) on pre-coated silica gel G plates at 254 nm under a UV lamp. Column chromatography separations were performed on silica gel (200–300 mesh).

4.1.1 Synthesis of 3-hydroxymethylindazole (**7**)

LiAlH_4 (1.176 g, 31.0 mmol) was added in portions to a solution of 1*H*-indazole-3-carboxylic acid (2.506 g, 15.5 mmol) in anhydrous THF (70 mL) at 0–5 °C. The resulting solution was stirred for 4 h at room temperature and then the reaction was quenched by the addition of 2 mL water, HCl (1 M) at ice bath. Then, celite was added, and the resulting mixture was stirred for 5 min. The mixture was filtered, and the filtrate was concentrated to remove most of solvent. The residue was extracted with ethyl acetate. The combined organic layers were washed with water, dried over anhydrous sodium sulfate, and concentrated under vacuum to get 3-hydroxymethylindazole (**7**) as a light brown solid (1.65 g) in a yield of 72%, ^1H NMR (DMSO- d_6 , 400 MHz) δ 12.79 (s, 1H, IndNH), 7.85–7.83 (d, 1H, ArH), 7.49–7.47 (d, 1H, ArH), 7.35–7.31 (t, 1H, ArH), 7.11–7.07 (t, 1H, ArH), 5.24–5.21 (t, 1H, OH), 4.80–4.78 (d, 2H, $-\text{CH}_2-$).

4.1.2 Synthesis of 1-Boc-3-hydroxymethylindazole (**8**)

Triethylamine (1.5 mL, 11.0 mmol), DMAP (0.182 g, 1.5 mmol), and Boc_2O (1.610 g, 7.4 mmol) were successively added to the solution of compound **7** (1.09 g, 7 mmol) in dry THF (70 mL), and the mixture was stirred at room temperature for 2 h. The solvent was removed under reduced pressure. Then the residue was dissolved in dichloromethane (80 mL). The solution was washed with water (2×50 mL), dried over anhydrous sodium sulfate and then concentrated in vacuum. The crude product was purified by column chromatography using gradient elution (EA/PE = 8:1 to 4:1) to give **8** (0.9 g, 49.3%). ^1H NMR (DMSO- d_6 , 400 MHz) δ 8.08–8.06 (d, 1H, ArH), 7.97–7.95 (d, 1H, ArH), 7.60–7.56 (t, 1H, ArH), 7.38–7.34 (t, 1H, ArH), 5.56 (s, 1H, OH), 4.82–4.81 (d, 2H, $-\text{CH}_2-$), 1.63 (s, 9H, $-\text{COOC}(\text{CH}_3)_3$).

4.1.3 Synthesis of 1-Boc-3-bromomethylindazole (**9**)

Compound **8** (0.9 g, 3.6 mmol) was dissolved in anhydrous DMF (35 mL). PBr_3 (0.69 mL, 7.3 mmol) was added slowly and the mixture was stirred for 1 h at room temperature. 1 M sodium hydroxide solution (50 mL) was added, and the mixture was extracted with ethyl acetate (70 mL). The organic layer was washed with H_2O (2×50 mL), dried over anhydrous sodium sulfate and concentrated under reduced pressure. The crude product was purified by column chromatography (EA:PE = 1:20) to afford **9** (0.7 g, 62.1%) as a white solid. ^1H NMR (DMSO- d_6 , 400 MHz) δ 8.10–8.08 (d, 1H, ArH), 7.97–7.95 (d, 1H, ArH), 7.66–7.62 (t, 1H, ArH), 7.46–7.43 (t, 1H, ArH), 5.05 (s, 2H, $-\text{CH}_2-$), 1.65 (s, 9H, $-\text{COOC}(\text{CH}_3)_3$).

4.1.4 Synthesis of intermediates **11a-q**

A reaction mixture of 2-chlorophenol (1.726 g, 13.4 mmol) and sodium hydroxide in *N,N*-dimethylformamide (30 ml) was stirred at ice bath for 5 min. Then 2,4-dichloropyrimidine (2.005 g, 13.5 mmol) was added to the solution and continued to stir for 2 h at room temperature (monitored by TLC). After completion of the reaction, the mixture was poured slowly to the ice brine (100 ml) under vigorous stirring, the precipitates was gathered by filtration, washed with ice water (3 × 10 ml) and dried to get 2-chloro-4-(2-chlorophenoxy)pyrimidine **11a** as a white solid (2.787 g, yield 75.4%), which was used directly in the next step without further purification.

The compounds **11b-q** were prepared using the same method.

4.1.5 Synthesis of intermediates **12a-q**

A mixture of 2-chloro-4-(2-chlorophenoxy)pyrimidine **11a** (2.502 g, 10.4 mmol), 4-amino-1-Boc-piperidine (2.500 g, 12.5 mmol) and DIEA (3.4 mL, 20.6 mmol) in *N*-methylpyrrolidone (40 mL) was slowly heated at 100 °C for 4h under argon. The reaction mixture was cooled to room temperature and poured into water and extracted with ethyl acetate (100 ml). Then organic layer was washed with brine (3 × 80 ml), dried over anhydrous sodium sulfate and concentrated under reduced pressure to get crude product, which was purified by column chromatography using gradient elution (EA/PE = 8:1 to 3:1, v/v, containing 1% TEA) to obtain **12a**.

The compounds **12b-q** were prepared using the same method.

12a: white solid, yield 37.6%; ¹H NMR (CDCl₃, 600 MHz) δ 8.14-8.13 (d, 1H, PyH₆), 7.45-7.17 (m, 4H, PhH), 6.15-6.14 (d, 1H, PyH₅), 5.11 (brs, 1H, NH), 3.96-3.45 (m, 3H, PipH), 2.71 (s, 2H, PipH), 1.87 (s, 2H, PipH), 1.44 (s, 9H, 3CH₃), 1.28-1.25 (m, 2H, PipH).

12b: white solid, yield 37.3%; ¹H NMR (CDCl₃, 400 MHz) δ 8.13 (s, 1H, PyH₆), 7.34-6.89 (m, 4H, PhH), 6.12-6.10 (d, 1H, PyH₅), 5.30 (brs, 1H, NH), 3.97 (s, 2H, PipH), 2.81 (s, 2H, PipH), 1.92-1.90 (m, 2H, PipH), 1.44 (s, 9H, C(CH₃)₃), 1.35-1.30 (m, 3H, PipH).

12c: white solid, yield 44.2%; ¹H NMR (CDCl₃, 400 MHz) δ 8.11 (s, 1H, PyH₆), 7.36-7.06 (m, 4H, PhH), 6.10-6.09 (d, 1H, PyH₅), 5.65-4.85 (brd, 1H, NH), 3.98 (s, 2H, PipH), 2.83 (s, 2H, PipH), 1.91 (s, 2H, PipH), 1.44 (s, 9H, C(CH₃)₃), 1.36-1.30 (m, 3H, PipH).

12d: white solid, yield 45.1%; ¹H NMR (CDCl₃, 400 MHz) δ 8.10-8.09 (d, 1H, PyH₆), 7.60-7.08 (m, 4H, PhH), 6.13-6.12 (d, 1H, PyH₅), 5.41 (brs, 1H, NH), 3.93 (s, 2H, PipH), 2.69 (s, 2H, PipH), 1.84 (s, 2H, PipH), 1.42 (s, 9H, C(CH₃)₃), 1.26-1.23 (m, 3H, PipH).

12e: white solid, yield 33.0%; ¹H NMR (CDCl₃, 400 MHz) δ (ppm): 8.15-8.14 (d, 1H, PyH₆), 7.38-7.08 (m, 4H, PhH), 6.15-6.14 (d, 1H, PyH₅), 5.35 (brs, 1H, NH), 4.04-3.75 (m, 3H, PipH), 2.84 (s, 2H, PipH), 1.96-1.93 (m, 2H, PipH), 1.47 (s, 9H, C(CH₃)₃), 1.38-1.30 (m, 2H, PipH).

12f: white solid, yield 33.9%; ¹H NMR (CDCl₃, 400 MHz) δ 8.11-8.10 (d, 1H, PyH₆), 7.50-7.48 (d, 2H, PhH), 7.02-7.00 (d, 2H, PhH), 6.09-6.08 (d, 1H, PyH₅), 5.53-4.92 (brd, 1H, NH), 3.98-3.75 (m, 3H, PipH), 2.82 (s, 2H, PipH), 1.91 (s, 2H, PipH), 1.44 (s, 9H, C(CH₃)₃), 1.34-1.29 (m, 2H, PipH).

12g: white solid, yield 44%; $^1\text{H NMR}$ (CDCl_3 , 400 MHz) δ 8.17-8.16 (d, 1H, PyH_6), 7.73-7.28 (m, 4H, PhH), 6.24-6.23 (d, 1H, PyH_5), 5.26 (brs, 1H, NH), 3.97 (s, 2H, PipH), 2.77 (s, 2H, PipH), 1.88 (s, 2H, PipH), 1.47 (s, 9H, $\text{C}(\text{CH}_3)_3$), 1.31-1.29 (m, 3H, PipH).

12h: white solid, yield 36.3%; $^1\text{H NMR}$ (CDCl_3 , 400 MHz) δ 8.13-8.12 (d, 1H, PyH_6), 7.53-7.30 (m, 4H, PhH), 6.16-6.15 (d, 1H, PyH_5), 5.50 (brs, 1H, NH), 3.95 (s, 2H, PipH), 2.73 (s, 2H, PipH), 1.86 (s, 2H, PipH), 1.43 (s, 9H, $\text{C}(\text{CH}_3)_3$), 1.32-1.24 (m, 3H, PipH).

12i: white solid, yield 27.6%; $^1\text{H NMR}$ (CDCl_3 , 400 MHz) δ 8.13 (s, 1H, PyH_6), 7.65-7.22 (m, 4H, PhH), 6.15-6.13 (d, 1H, PyH_5), 5.62-4.86 (brd, 1H, NH), 3.95 (s, 3H, PipH), 2.78 (s, 2H, PipH), 1.88 (s, 2H, PipH), 1.42 (s, 9H, $\text{C}(\text{CH}_3)_3$), 1.30-1.27 (m, 2H, PipH).

12j: yellow oil, yield 44.8%; $^1\text{H NMR}$ (CDCl_3 , 400 MHz) δ 7.99-7.98 (d, 1H, PyH_6), 7.18-6.82 (d, 4H, PhH), 5.94-5.92 (d, 1H, PyH_5), 3.91-3.69 (m, 3H, PipH), 2.71 (s, 2H, PipH), 2.26 (s, 3H, CH_3), 1.86-1.83 (d, 2H, PipH), 1.37 (s, 9H, $\text{C}(\text{CH}_3)_3$), 1.27-1.20 (m, 2H, PipH).

12k: white solid, yield 39.2%; $^1\text{H NMR}$ (CDCl_3 , 400 MHz) δ 8.07-8.06 (d, 1H, PyH_6), 7.18-6.98 (m, 4H, PhH), 6.01-5.99 (d, 1H, PyH_5), 5.39 (brs, 1H, NH), 3.98-3.82 (m, 3H, PipH), 2.82 (s, 2H, PipH), 2.35 (s, 3H, CH_3), 1.94-1.92 (d, 2H, PipH), 1.44 (s, 9H, $\text{C}(\text{CH}_3)_3$), 1.32-1.29 (m, 2H, PipH).

12l: white solid, yield 30.6%; $^1\text{H NMR}$ (CDCl_3 , 400 MHz) δ 8.09-8.08 (d, 1H, PyH_6), 7.46-7.33 (m, 4H, PhH), 6.12-6.10 (d, 1H, PyH_5), 5.08 (brs, 1H, NH), 3.93 (s, 2H, PipH), 2.71 (s, 2H, PipH), 1.82 (s, 2H, PipH), 1.39 (s, 9H, $\text{C}(\text{CH}_3)_3$), 1.26-1.22 (m, 3H, PipH).

12m: white solid, yield 21.5%; $^1\text{H NMR}$ (CDCl_3 , 400 MHz) δ 8.17-8.15 (d, 1H, PyH_6), 7.70-7.24 (m, 4H, PhH), 6.19-6.17 (d, 1H, PyH_5), 5.46-4.94 (brd, 1H, NH), 3.97-3.79 (m, 3H, PipH), 2.81 (s, 2H, PipH), 1.89 (s, 2H, PipH), 1.44 (s, 9H, $\text{C}(\text{CH}_3)_3$), 1.35-1.26 (m, 2H, PipH).

12n: white solid, yield 35.9%; $^1\text{H NMR}$ (CDCl_3 , 400 MHz) δ 8.08-8.07 (d, 1H, PyH_6), 7.06 (s, 3H, PhH), 5.99-5.98 (d, 1H, PyH_5), 5.45-4.98 (brd, 1H, NH), 3.97-3.68 (m, 3H, PipH), 2.79 (s, 2H, PipH), 2.11 (s, 6H, 2CH_3), 1.89 (s, 2H, PipH), 1.44 (s, 9H, $\text{C}(\text{CH}_3)_3$), 1.32-1.25 (m, 2H, PipH).

12o: white oil, yield 23.9%; $^1\text{H NMR}$ (CDCl_3 , 400 MHz) δ 8.17-8.16 (d, 1H, PyH_6), 7.49-7.38 (s, 3H, PhH), 6.20-6.18 (d, 1H, PyH_5), 5.70-4.86 (brd, 1H, NH), 3.99 (s, 3H, PipH), 2.78 (s, 2H, PipH), 1.89 (s, 2H, PipH), 1.43 (s, 9H, $\text{C}(\text{CH}_3)_3$), 1.35-1.31 (m, 2H, PipH).

12p: white oil, yield 46.2%; $^1\text{H NMR}$ (CDCl_3 , 400 MHz) δ 7.97(s, 1H, PyH_6), 6.77 (s, 2H, PhH), 5.92-5.91 (d, 1H, PyH_5), 5.17(brs, 1H, NH), 3.91-3.62 (s, 3H, PipH), 2.68 (s, 2H, PipH), 2.55 (s, 6H, 2CH_3), 1.83-1.81 (s, 2H, PipH), 1.35 (s, 9H, $\text{C}(\text{CH}_3)_3$), 1.23-1.20 (m, 2H, PipH).

12q: white solid, yield 63.7%; $^1\text{H NMR}$ (CDCl_3 , 400 MHz) δ 7.96 (s, 1H, PyH_6), 7.26 (s, 2H, PhH), 6.01-6.00 (d, 1H, PyH_5), 3.80 (s, 2H, PipH), 2.60 (s, 2H, PipH), 2.01 (s, 6H, 2CH_3), 1.91-1.89 (d, 1H, NH), 1.66(s, 2H, PipH), 1.31 (s, 9H, $\text{C}(\text{CH}_3)_3$), 1.15-1.09 (m, 3H, PipH).

4.1.6 Synthesis of intermediates **13a-q**

Trifluoroacetic acid (2.8 mL, 37.7 mmol) was added to a solution of **12a** (1.52 g, 3.4 mmol) in dichloromethane (30 mL) in ice bath for 0.5 h, then the ice bath was removed. The mixture was stirred for 3 h. After completion of the reaction, the reaction mixture was alkalized with saturated

sodium bicarbonate solution until no gas bubbled. The aqueous layer was extracted with dichloromethane (1 × 50 ml) and washed with water (2 × 50 ml). The organic layer was dried over anhydrous sodium sulfate, filtered, and concentrated under reduced pressure to obtain **13a** (1.101 g, yield 96.2%). The crude product was used directly for the next step.

The intermediates **13b-q** were prepared using the same method.

4.1.7 Synthesis of intermediates **14a-q**

Compound **13a** (0.707 g, 2.3 mmol), **9** (0.789 g, 2.5 mmol) and 18-Crown-6 (0.061 g, 0.23 mmol) were dissolved in tetrahydrofuran (18 mL) in the presence of anhydrous potassium carbonate, the mixture was stirred at room temperature for 4 h. After completion of the reaction, water (80 ml) and ethyl acetate (80 mL) was added for extraction. The organic layer was washed with brine (2 × 80 ml), then dried over anhydrous sodium sulfate to obtain the corresponding crude product, which was purified by column chromatography using gradient elution (EA/PE = 3:1 to 1:1, v/v, containing 1% TEA) to afford **14a** (0.47g, yield 38.1%) as white grease.

The intermediates **14b-q** were prepared using the same method.

4.1.8 Synthesis of intermediates **5a-q**

Trifluoroacetic acid (1.2 mL, 16.1 mmol) was added to a solution of **14a** (0.418 g, 0.8 mmol) in dichloromethane (10 mL) in ice bath and stirred for 0.5 h. Then the ice bath was removed, and the mixture was stirred for another 3 h (monitored by TLC). Then, the reaction solution was alkalized with saturated sodium bicarbonate solution until no gas bubble. The aqueous phase was extracted with dichloromethane (60 ml) and washed with water (2 × 50 ml). The organic phase was dried over anhydrous sodium sulfate, filtered, and concentrated under reduced pressure. The crude product was purified by stirring and rinsing with a mixed solvent (*n*-hexane/dichloromethane, 6:1, v/v) to obtain **5a**.

The compounds **5b-q** were prepared using the same method.

5a: *n*-hexane/dichloromethane (6:1, v/v), white solid, yield 52.9%, mp 182.9-187.3°C; ¹H NMR (400 MHz, DMSO-*d*₆) δ 12.80 (s, 1H, IndNH), 8.16 (s, 1H, PyH₆), 7.84-7.07 (m, 8H, ArH), 6.19-6.18 (d, 1H, PyH₅), 3.79-3.70 (m, 3H, -CH₂- and PipH), 2.84-2.79 (m, 2H, PipH), 2.07-1.34 (m, 6H, PipH); ¹³C NMR (200 MHz, DMSO-*d*₆): δ 168.55, 161.63, 160.27, 159.84, 148.25, 140.87, 130.32, 128.55, 126.99, 126.47, 125.86, 124.54, 122.15, 120.60, 119.72, 110.03, 95.82, 54.41, 52.09, 48.33, 31.04; HRMS (ESI+) calcd for C₂₃H₂₃ClN₆O: 435.1622. Found: 435.1698 (M+H)⁺.

5b: *n*-hexane/dichloromethane (10:1, v/v), white solid, yield 57.6%, mp 154.3-156.8°C; ¹H NMR (400 MHz, DMSO-*d*₆) δ 12.78 (s, 1H, IndNH), 8.15 (s, 1H, PyH₆), 7.84-7.01 (m, 8H, ArH), 6.14 (s, 1H, PyH₅), 3.78-3.69 (m, 3H, -CH₂- and PipH), 2.82 (s, 2H, PipH), 2.04-1.42 (m, 6H, PipH); ¹³C NMR (200 MHz, DMSO-*d*₆): δ 168.90, 161.60, 160.35, 159.88, 153.22, 142.28, 140.88, 133.53, 130.67, 125.84, 125.34, 122.15, 120.62, 119.68, 118.04, 110.01, 96.32, 54.55, 52.24, 48.02, 31.28; MS (ESI+) calcd for C₂₃H₂₃ClN₆O: 435.16. Found: 435.99 (M+H)⁺.

5c: *n*-hexane/dichloromethane (8:1, v/v), white solid, yield 51.9%, mp 194.3-196.4°C; ¹H

NMR (400 MHz, DMSO- d_6) δ 12.80 (s, 1H, IndNH), 8.14 (s, 1H, PyH₆), 7.84-7.05 (m, 8H, ArH), 6.15-6.10 (d, 1H, PyH₅), 3.77-3.67 (m, 3H, -CH₂- and PipH), 2.81 (s, 2H, PipH), 2.03-1.40 (m, 6H, PipH); ¹³C NMR (200 MHz, DMSO- d_6) δ 169.04, 161.67, 159.79, 151.17, 142.34, 140.89, 129.53, 129.25, 125.82, 123.81, 122.12, 120.60, 119.66, 110.01, 96.25, 54.62, 52.42, 48.02, 31.40; HRMS (ESI+) calcd for C₂₃H₂₃ClN₆O: 435.1622. Found: 435.1715 (M+H)⁺.

5d: *n*-hexane/dichloromethane (6:1, v/v), white solid, yield 76.4%, mp 163.5-166.7°C; ¹H NMR (400 MHz, DMSO- d_6) δ 12.81 (s, 1H, IndNH), 8.16 (s, 1H, PyH₆), 7.84-7.06 (m, 8H, ArH), 6.17-6.16 (d, 1H, PyH₅), 3.79-3.69 (m, 3H, -CH₂- and PipH), 2.84-2.80 (m, 2H, PipH), 2.08-1.34 (m, 6H, PipH); ¹³C NMR (200 MHz, DMSO- d_6): δ 168.54, 161.63, 160.23, 149.49, 142.09, 140.87, 133.31, 129.13, 127.29, 125.85, 124.55, 122.15, 120.59, 119.71, 115.98, 110.03, 95.94, 54.41, 52.40, 47.92, 31.07; HRMS (ESI+) calcd for C₂₃H₂₃BrN₆O: 479.1117, 481.1096. Found: 479.1192, 481.1171 (M+H)⁺.

5e: *n*-hexane/dichloromethane (8:1, v/v), white solid, yield 76.4%, mp 152.1-155.5°C; ¹H NMR (400 MHz, DMSO- d_6) δ 12.85 (s, 1H, IndNH), 8.15 (s, 1H, PyH₆), 7.85-7.07 (m, 8H, ArH), 6.15 (s, 1H, PyH₅), 3.85-3.70 (m, 3H, -CH₂- and PipH), 2.88 (s, 2H, PipH), 2.12-1.44 (m, 6H, PipH); ¹³C NMR (200 MHz, DMSO- d_6): δ 168.84, 161.41, 160.33, 159.85, 153.00, 140.86, 131.38, 128.22, 125.88, 124.95, 122.19, 121.74, 121.23, 120.56, 119.78, 110.06, 96.39, 54.19, 52.21, 48.04, 31.05; HRMS (ESI+) calcd for C₂₃H₂₃BrN₆O: 479.1117, 481.1096. Found: 479.1168, 481.1151 (M+H)⁺.

5f: *n*-hexane/dichloromethane (6:1, v/v), light yellow solid, yield 35.3%, mp 194.3-196.8°C; ¹H NMR (400 MHz, DMSO- d_6) δ 12.80 (s, 1H, IndNH), 8.14 (s, 1H, PyH₆), 7.84-7.06 (m, 8H, ArH), 6.15-6.10 (d, 1H, PyH₅), 3.77-3.67 (m, 3H, -CH₂- and PipH), 2.82 (s, 2H, PipH), 2.03-1.40 (m, 6H, PipH); ¹³C NMR (200 MHz, DMSO- d_6): δ 168.96, 161.38, 159.80, 151.66, 142.30, 140.88, 132.48, 125.83, 124.25, 122.11, 120.59, 119.67, 117.35, 110.01, 96.27, 54.59, 52.39, 47.99, 31.37; HRMS (ESI+) calcd for C₂₃H₂₃BrN₆O: 479.1117, 481.1096. Found: 479.1211, 481.1196 (M+H)⁺.

5g: *n*-hexane/dichloromethane (8:1, v/v), white solid, yield 46.4%, mp 193.5-195.8°C; ¹H NMR (400 MHz, DMSO- d_6) δ 12.79 (s, 1H, IndNH), 8.17 (s, 1H, PyH₆), 7.83-7.06 (m, 8H, ArH), 6.21-6.20 (d, 1H, PyH₅), 3.77-3.69 (m, 2H, -CH₂- and PipH), 2.83-2.77 (m, 2H, PipH), 2.05-1.35 (m, 6H, PipH); ¹³C NMR (200 MHz, DMSO- d_6): δ 169.06, 161.38, 160.37, 149.87, 142.20, 140.88, 133.46, 126.85, 125.84, 125.70, 124.80, 123.86, 122.51, 122.14, 120.61, 119.67, 110.01, 96.17, 54.51, 52.41, 48.03, 31.33; HRMS (ESI+) calcd for C₂₄H₂₃F₃N₆O: 469.1885. Found: 469.1943 (M+H)⁺.

5h: *n*-hexane/dichloromethane (6:1, v/v), white solid, yield 37.3%, mp 158.5-161.7°C; ¹H NMR (400 MHz, DMSO- d_6) δ 12.78 (s, 1H, IndNH), 8.17 (s, 1H, PyH₆), 7.82-7.06 (m, 8H, ArH), 6.20-6.19 (d, 1H, PyH₅), 3.76 (s, 3H, -CH₂- and PipH), 2.78 (s, 2H, PipH), 2.08-1.38 (m, 6H, PipH); ¹³C NMR (200 MHz, DMSO- d_6): δ 168.73, 161.41, 160.12, 152.57, 142.11, 140.82, 130.59, 125.99, 125.66, 124.29, 122.93, 122.05, 121.65, 120.43, 119.52, 118.98, 109.88, 96.28, 54.43, 52.12, 48.03, 31.17; HRMS (ESI+) calcd for C₂₄H₂₃F₃N₆O: 469.1885. Found: 469.1887 (M+H)⁺.

5i: *n*-hexane/dichloromethane (6:1, v/v), white solid, yield 65.5%, mp 169.2-173.6°C; ¹H

NMR (400 MHz, DMSO- d_6) δ 13.65 (s, 1H, IndNH), 10.58-10.45 (d, 1H, -NH-); 8.24-8.23 (d, 1H, PyH₆), 8.02-7.19 (m, 8H, ArH), 6.34-6.33 (d, 1H, PyH₅), 4.65(s, 2H, -CH₂-), 4.06-3.90 (m, 1H, PipH), 3.53 (s, 2H, PipH), 3.24-2.94 (m, 2H, PipH), 2.00-1.72 (m, 4H, PipH); ¹³C NMR (200 MHz, DMSO- d_6): δ 168.76, 160.93, 159.53, 158.15, 155.30, 140.73, 134.42, 126.84, 126.37, 122.55, 122.42, 120.87, 119.94, 115.62, 110.46, 97.14, 54.76, 50.75, 47.19, 28.27; HRMS (ESI+) calcd for C₂₄H₂₃F₃N₆O: 469.1885. Found: 469.1984 (M+H)⁺.

5j: *n*-hexane/dichloromethane (6:1, v/v), white solid, yield 62.7%, mp 135.8-139.4□; ¹H NMR (400 MHz, DMSO- d_6) δ 12.81 (s, 1H, IndNH), 8.11 (s, 1H, PyH₆), 7.85-6.92 (m, 8H, ArH), 6.04 (s, 1H, PyH₅), 3.82-3.69(m, 3H, -CH₂- and PipH), 2.84 (s, 2H, PipH), 2.28 (s, 3H, -CH₃-), 2.07-1.43 (m, 6H, PipH); ¹³C NMR (200 MHz, DMSO- d_6): δ 169.26, 161.62, 159.62, 152.30, 141.90, 140.82, 139.08, 129.09, 125.70, 125.65, 122.11, 122.05, 120.44, 119.59, 118.48, 109.91, 96.02, 54.27, 52.10, 47.85, 31.15, 20.67; HRMS (ESI+) calcd for C₂₄H₂₆N₆O: 415.2168. Found: 415.2267 (M+H)⁺.

5k: *n*-hexane/dichloromethane (10:1, v/v), white solid, yield 77.6%, mp 141.1-145.6□; ¹H NMR (400 MHz, DMSO- d_6) δ 13.12 (s, 1H, IndNH), 8.12-8.11 (d, 1H, PyH₆), 7.91-7.01 (m, 8H, ArH), 6.06 (s, 1H, PyH₅), 4.11(s, 2H, -CH₂-), 3.06 (s, 2H, PipH), 2.29 (s, 3H, -CH₃-); 1.82-1.24 (m, 7H, PipH); ¹³C NMR (200 MHz, DMSO- d_6): δ 169.54, 161.52, 160.04, 159.57, 150.10, 140.83, 134.35, 130.05, 129.86, 126.09, 122.35, 120.41, 120.18, 110.23, 96.40, 54.93, 51.67, 47.29, 30.18, 20.38; HRMS (ESI+) calcd for C₂₄H₂₆N₆O: 415.2168. Found: 415.2264 (M+H)⁺.

5l: *n*-hexane/dichloromethane (8:1, v/v), white solid, yield 64.4%, mp 170.9-173.2□; ¹H NMR (400 MHz, DMSO- d_6): δ 12.78 (s, 1H, IndNH), 8.17 (s, 1H, PyH₆), 7.84-7.07 (m, 8H, ArH), 6.20-6.19 (d, 1H, PyH₅), 3.79-3.68 (m, 3H, -CH₂- and PipH), 2.82 (s, 2H, PipH), 2.05-1.40 (m, 6H, PipH); ¹³C NMR (200 MHz, DMSO- d_6): δ 168.67, 161.47, 160.48, 152.41, 142.19, 140.88, 131.07, 129.20, 127.39, 125.84, 122.13, 120.61, 119.69, 118.08, 112.39, 110.02, 96.36, 54.53, 52.36, 47.98, 28.53; HRMS (ESI+) calcd for C₂₄H₂₃N₇O: 426.1964. Found: 426.2049 (M+H)⁺.

5m: *n*-hexane/dichloromethane (6:1, v/v), white solid, yield 54%, mp 202.2-205.1□; ¹H NMR (400 MHz, DMSO- d_6) δ 12.78 (s, 1H, IndNH), 8.19 (s, 1H, PyH₆), 7.91-7.06 (m, 8H, ArH), 6.21 (s, 1H, PyH₅), 3.79-3.71 (m, 3H, -CH₂- and PipH), 2.83 (s, 2H, PipH), 2.06-1.39 (m, 6H, PipH); ¹³C NMR (200 MHz, DMSO- d_6): δ 168.49, 161.35, 160.23, 156.17, 142.22, 140.88, 134.16, 125.85, 122.98, 122.12, 120.58, 119.70, 118.52, 110.03, 107.74, 96.57, 54.58, 52.31, 48.02, 31.33; HRMS (ESI+) calcd for C₂₄H₂₃N₇O: 426.1964. Found: 426.2028 (M+H)⁺.

5n: *n*-hexane/dichloromethane (6:1, v/v), white solid, yield 52.3%, mp 163.5-167.4□; ¹H NMR (400 MHz, DMSO- d_6): δ 12.80 (s, 1H, IndNH), 8.11 (s, 1H, PyH₆), 7.83-7.05 (m, 7H, ArH), 6.03 (s, 1H, PyH₅), 3.76-3.67 (m, 3H, -CH₂- and PipH), 2.81-2.75 (m, 2H, PipH), 2.02 (s, 7H, -CH₃- and PipH), 1.75-1.33 (m, 5H, PipH); ¹³C NMR (200 MHz, DMSO- d_6): δ 168.49, 161.73, 159.86, 149.29, 142.31, 140.88, 130.23, 128.64, 125.82, 125.32, 122.12, 120.62, 119.64, 109.99, 94.48, 54.59 52.43, 48.06, 31.40, 16.07; MS (ESI+) calcd for C₂₅H₂₈N₆O: 429.23. Found: 429.74 (M+H)⁺.

5o: *n*-hexane/dichloromethane (6:1, v/v), white solid, yield 53.8%, mp 167.1-169.8□; ¹H NMR (400 MHz, DMSO- d_6): δ 12.78 (s, 1H, IndNH), 8.19 (s, 1H, PyH₆), 7.90-7.06 (m, 7H, ArH),

6.24-6.23 (d, 1H, PyH₅), 3.78-3.70 (m, 2H, -CH₂- and PipH), 2.82 (m, 2H, PipH), 2.04-1.41 (m, 6H, PipH); ¹³C NMR (200 MHz, DMSO-*d*₆): δ 168.46, 161.36, 160.15, 153.06, 142.14, 140.87, 134.27, 128.54, 127.98, 125.81, 125.05, 122.15, 120.60, 119.68, 116.91, 113.27, 110.02, 96.32, 54.51, 52.40, 48.07, 31.22; HRMS (ESI+) calcd for C₂₄H₂₂ClN₇O: 460.1574. Found: 460.1660 (M+H)⁺.

5p: *n*-hexane/dichloromethane (6:1, v/v), white solid, yield 62.3%, mp 198.3-200.5 °C; ¹H NMR (400 MHz, DMSO-*d*₆): δ 12.80 (s, 1H, IndNH), 8.12 (s, 1H, PyH₆), 7.83-7.03 (m, 6H, ArH), 6.11-6.07 (d, 1H, PyH₅), 3.77-3.67 (m, 2H, -CH₂- and PipH), 2.82 (s, 2H, PipH), 2.30 (s, 6H, 2CH₃), 2.02-1.40 (m, 6H, PipH); ¹³C NMR (200 MHz, DMSO-*d*₆): δ 169.07, 161.50, 159.64, 150.31, 142.31, 140.85, 137.06, 129.96, 125.81, 122.14, 121.96, 120.56, 119.66, 110.00, 96.13, 54.54, 52.46, 48.02, 31.39, 20.23; HRMS (ESI+) calcd for C₂₅H₂₇ClN₆O: 463.1935. Found: 463.2015 (M+H)⁺.

5q: column chromatography on silica gel (ethyl acetate), white solid, yield 42%, mp 160.7-164.5 °C; ¹H NMR (400 MHz, DMSO-*d*₆): δ 12.80 (s, 1H, IndNH), 8.17 (s, 1H, PyH₆), 7.83-7.03 (m, 6H, ArH), 6.20 (s, 1H, PyH₅), 3.76-3.65 (m, 3H, -CH₂- and PipH), 2.81-2.74 (m, 2H, PipH), 2.06 (s, 6H, -CH₃-), 1.98-1.29 (m, 6H, PipH); ¹³C NMR (200 MHz, DMSO-*d*₆): δ 167.79, 161.51, 160.04, 153.23, 142.32, 140.88, 132.66, 132.13, 125.82, 122.09, 120.58, 119.66, 118.62, 110.01, 108.13, 95.22, 54.58, 52.42, 48.07, 31.36, 15.87; HRMS (ESI+) calcd for C₂₆H₂₇N₇O: 454.2277. Found: 454.2341 (M+H)⁺.

4.2. Anti-HIV activity and cytotoxicity assay in MT-4 cells

The anti-HIV activities and cytotoxicities of the target molecules were evaluated against wild-type (WT) HIV-1 strain IIIB, common single mutants K103N, Y181C, E138K, double mutant (K103N+Y181C) (RES056) and HIV-2 strain (ROD) in MT-4 cell cultures using the 3-(4,5-dimethylthiazol-2-yl)-2,5-diphenyltetrazolium bromide (MTT) method [28,29]. Briefly, stock solutions (10 × final concentration) of test compounds were added in 25 μL volumes to two series of triplicate wells so as to allow simultaneous evaluation of their effects on mock- and HIV-infected cells at the beginning of each experiment. Serial 5-fold dilutions of test compounds were made directly in flat-bottomed 96-well microtiter trays using a Biomek 3000 robot (Beckman instruments, Fullerton, CA). Untreated control HIV- and mock-infected cell samples were included for each sample. Virus stock (50 μL) at 100–300 CCID₅₀ (50% cell culture infectious dose) or culture medium was added to either the virus-infected or mock-infected wells of the microtiter tray. Mock-infected cells were used to evaluate the effect of test compounds on uninfected cells in order to assess the cytotoxicity of the test compounds. Exponentially growing MT-4 cells were centrifuged for 5 min at 1000 rpm (220 g) and the supernatant was discarded. The MT-4 cells were resuspended at 6 × 10⁵ cells/mL and 50-μL volumes were transferred to the microtiter tray wells. Five days after infection, the viability of mock- and HIV-infected cells was examined spectrophotometrically by the MTT assay.

The MTT assay is based on the reduction of yellow colored 3-(4,5-dimethylthiazol-2-yl)-2,5-diphenyltetrazolium bromide (MTT) (Acros Organics) by mitochondrial dehydrogenase

activity in metabolically active cells to a blue-purple formazan that can be measured spectrophotometrically. The absorbances were read in an eight-channel computer-controlled photometer (Infinite M1000, Tecan), at two wavelengths (540 and 690 nm). All data were calculated using the median absorbance value of three wells. The 50% cytotoxic concentration (CC_{50}) was defined as the concentration of the test compound that reduced the absorbance (OD_{540}) of the mock-infected control sample by 50%. The concentration achieving 50% protection against the cytopathic effect of the virus in infected cells was defined as the 50% effective concentration (EC_{50}).

4.3. Molecular docking

Molecular docking was performed with the Tripos molecular modeling packages Sybyl-X 1.2. All the molecules for docking were built using standard bond lengths and angles from Sybyl-X 1.2/base Builder and were then optimized using the Tripos force field for 2000 generations two times or more, until the minimized conformers of the ligand were the same. The flexible docking method, called Surflex-Dock, docks the ligand automatically into the ligand binding site of the receptor by using a protocol-based approach and an empirically-derived scoring function [31-33]. The protocol is a computational representation of a putative ligand that binds to the intended binding site and is a unique and essential element of the docking algorithm. The scoring function in Surflex-Dock, which contains hydrophobic, polar, repulsive, entropic, and solvation terms, was trained to estimate the dissociation constant (K_d) expressed in $-\log(K_d)^2$. Prior to docking, the protein was prepared by removing water molecules, the ligand **3c**, and other unnecessary small molecules from the crystal structure of the **3c**-HIV-1 RT complex (PDB code: 3NBP) [30]; simultaneously, polar hydrogen atoms were added to the protein. Surflex-Dock default settings were used for other parameters, such as the number of starting conformations per molecule (set to 0), the size to expand search grid (set to 8 Å), the maximum number of rotatable bonds per molecule (set to 100), and the maximum number of poses per ligand (set to 20). During the docking procedure, all of the single bonds in residue side-chains inside the defined RT binding pocket were regarded as rotatable or flexible, and the ligand was allowed to rotate at all single bonds and move flexibly within the tentative binding pocket. The atomic charges were recalculated using the Kollman all-atom approach for the protein and the Gasteiger-Hückel approach for the ligand. The binding interaction energy was calculated to include van der Waals, electrostatic, and torsional energy terms defined in the Tripos force field. The structure optimization was performed for 20,000 generations using a genetic algorithm, and the 20-best-scoring ligand-protein complexes were kept for further analyses. The $-\log(K_d)^2$ values of the 20-best-scoring complexes, which represented the binding affinities of ligand with RT, encompassed a wide scope of functional classes (10^{-2} - 10^{-9}). Therefore, only the highest-scoring 3D structural model of the ligand-bound RT was chosen to define the binding interaction [34-37].

Acknowledgments

The financial support from the National Natural Science Foundation of China (Nos. 21877087, 21602164, 21807082, 21402148), Wuhan International Scientific and Technological Cooperation Project (No. 2017030209020257), Natural Science Foundation of Hubei Province of China (No. 2017CFB121) and Hubei Provincial Department of Education of China (No. Q20171503) are greatly appreciated.

References

- [1] E. De Clercq, New developments in anti-HIV chemotherapy. *Curr. Med. Chem.* 8 (2001) 1543-1572.
- [2] Y. Mehellou, E. De Clercq, Twenty-six years of anti-HIV drug discovery: where do we stand and where do we go? *J. Med. Chem.* 53 (2010) 521-538.
- [3] V. Namasivayam, M. Vanangamudi, V.G. Kramer, S. Kurup, P. Zhan, X. Liu, J. Kongsted, S.N. Byrareddy, The journey of HIV-1 non-nucleoside reverse transcriptase inhibitors (NNRTIs) from lab to clinic. *J. Med. Chem.* 62 (2018) 4851-4883.
- [4] H.-H. Lu, P. Xue, Y.-Y. Zhu, X.-L. Ju, X.-J. Zheng, X. Zhang, T. Xiao, C. Pannecouque, T.-T. Li, S.-X. Gu, Structural modifications of diarylpyrimidines (DAPYs) as HIV-1 NNRTIs: synthesis, anti-HIV activities and SAR. *Bioorg. Med. Chem.* 25 (2017) 2491-2497.
- [5] P. Xue, H.-H. Lu, Y.-Y. Zhu, X.-L. Ju, C. Pannecouque, X.-J. Zheng, G.-Y. Liu, X.-L. Zhang, S.-X. Gu, Design and synthesis of hybrids of diarylpyrimidines and diketo acids as HIV-1 inhibitors. *Bioorg. Med. Chem. Lett.* 27 (2017) 1640-1643.
- [6] P. Shirvani, A. Fassihi, L. Saghaie, Recent advances in the design and development of nonnucleoside reverse transcriptase inhibitor scaffolds. *ChemMedChem* 14 (2019) 52-77.
- [7] K.R. Romines, G.A. Freeman, L.T. Schaller, J.R. Cowan, S.S. Gonzales, J.H. Tidwell, C.W. Andrews III, D.K. Stammers, R.J. Hazen, R.G. Ferris, S.A. Short, J.H. Chan, L.R. Boone, Structure-activity relationship studies of novel benzophenones leading to the discovery of a potent, next generation HIV nonnucleoside reverse transcriptase inhibitor. *J. Med. Chem.* 49 (2006) 727-739.
- [8] J.H. Chan, G.A. Freeman, J.H. Tidwell, K.R. Romines, L.T. Schaller, J.R. Cowan, S.S. Gonzales, C.W. Lowell, C. Andrews III, D.J. Reynolds, M.St. Clair, R.J. Hazen, R.G. Ferris, K.L. Creech, G.B. Roberts, S.A. Short, K. Weaver, G.W. Koszalka, L.R. Boone, Novel benzophenones as non-nucleoside reverse transcriptase inhibitors of HIV-1. *J. Med. Chem.* 47 (2004) 1175-1182.
- [9] S. Yang, F.-E. Chen, E. De Clercq, Dihydro-alkoxyl-benzyl-oxopyrimidine derivatives (DABOs) as non-nucleoside reverse transcriptase inhibitors: an update review (2001-2011). *Curr. Med. Chem.* 19 (2012) 152-162.
- [10] Y.-P. Wang, F.-E. Chen, E. De Clercq, J. Balzarini, C. Pannecouque, Synthesis and in vitro anti-HIV evaluation of a new series of 6-arylmethyl-substituted S-DABOs as potential non-nucleoside HIV-1 reverse transcriptase inhibitors. *Eur. J. Med. Chem.* 44 (2009) 1016-1023.
- [11] S.-X. Gu, X. Zhang, Q.-Q. He, L.-M. Yang, X.-D. Ma, Y.-T. Zheng, S.-Q. Yang, F.-E. Chen, Synthesis and biological evaluation of naphthyl phenyl ethers (NPEs) as novel nonnucleoside HIV-1 reverse transcriptase inhibitors. *Bioorg. Med. Chem.* 19 (2011) 4220-4226.

- [12] X. Chen, S. Ding, P. Zhan, X. Liu, Recent advances of diaryl ether family as HIV-1 non-nucleoside reverse transcriptase inhibitors. *Curr. Pharm. Design* 19 (2013) 2829-2838.
- [13] D.W. Ludovici, R.W. Kavash, M.J. Kukla, C.Y. Ho, H. Ye, B.L.D. Corte, K. Andries, M.-P. de Béthune, H. Azijn, R. Pauwels, H.E.L. Moereels, J. Heeres, L.M.H. Koymans, M.R. de Jonge, K.J.A. Van Aken, F.F.D. Daeyaert, P.J. Lewi, K. Das, E. Arnold, P.A.J. Janssen, Evolution of anti-HIV drug candidates. part 2:diaryltriazine (DATA) analogues. *Bioorg. Med. Chem. Lett.* 11 (2001) 2229-2234.
- [14] Y. Van Herrewege, G. Vanham, J. Michiels, K. Fransen, L. Kestens, K. Andries, P. Janssen, P. Lewi, A series of diaryltriazines and diarylpyrimidines are highly potent nonnucleoside reverse transcriptase inhibitors with possible applications as microbicides. *Antimicrob. Agents Chemother.* 48 (2004) 3684-3689.
- [15] S.-X. Gu, H.-H. Lu, G.-Y. Liu, X.-L. Ju, Y.-Y. Zhu, Advances in diarylpyrimidines and related analogues as HIV-1 nonnucleoside reverse transcriptase inhibitors. *Eur. J. Med. Chem.* 158 (2018) 371-392.
- [16] X. Chen, P. Zhan, D. Li, C.E. De, X. Liu, Recent advances in DAPYs and related analogues as HIV-1 NNRTIs. *Curr. Med. Chem.* 18 (2011) 359-376.
- [17] S.-X. Gu, Q.-Q. He, S.-Q. Yang, X.-D. Ma, F.-E. Chen, E. De Clercq, J. Balzarini, C. Pannecouque, Synthesis and structure-activity relationship of novel diarylpyrimidines with hydroxymethyl linker (*CH(OH)*-DAPYs) as HIV-1 NNRTIs. *Bioorg. Med. Chem.* 19 (2011) 5117-5124.
- [18] S.-X. Gu, S.-Q. Yang, Q.-Q. He, X.-D. Ma, F.-E. Chen, H.-F. Dai, E.D. Clercq, J. Balzarini, C. Pannecouque, Design, synthesis and biological evaluation of cycloalkyl arylpyrimidines (CAPYs) as HIV-1 NNRTIs. *Bioorg. Med. Chem.* 19 (2011) 7093-7099.
- [19] S.-X. Gu, Z.-M. Li, X.-D. Ma, S.-Q. Yang, Q.-Q. He, F.-E. Chen, E. De Clercq, J. Balzarini, C. Pannecouque, Chiral resolution, absolute configuration assignment and biological activity of racemic diarylpyrimidine *CH(OH)*-DAPY as potent nonnucleoside HIV-1 reverse transcriptase inhibitors. *Eur. J. Med. Chem.* 53 (2012) 229-234.
- [20] S.-X. Gu, Y.-Y. Zhu, F.-E. Chen, E. De Clercq, J. Balzarini, C. Pannecouque, Structural modification of diarylpyrimidine derivatives as HIV-1 reverse transcriptase inhibitors. *Med. Chem. Res.* 24 (2015) 220-225.
- [21] S.-X. Gu, H. Qiao, Y.-Y. Zhu, Q.-C. Shu, H. Liu, X.-L. Ju, E. De Clercq, J. Balzarini, C. Pannecouque, A novel family of diarylpyrimidines (DAPYs) featuring a diatomic linker: design, synthesis and anti-HIV activities. *Bioorg. Med. Chem.* 23 (2015) 6587-6593.
- [22] D.J. Kertesz, C. Brotherton-Pleiss, M. Yang, Z. Wang, X. Lin, Z. Qiu, D.R. Hirschfeld, S. Gleason, T. Mirzadegan, P.W. Dunten, Discovery of piperidin-4-yl-aminopyrimidines as HIV-1 reverse transcriptase inhibitors. *N*-Benzyl derivatives with broad potency against resistant mutant viruses. *Bioorg. Med. Chem. Lett.* 20 (2010) 4215-4218.
- [23] D.J. Kertesz, C. Brotherton-Pleiss, M. Yang, Z. Wang, X. Lin, Z. Qiu, D.R. Hirschfeld, S. Gleason, T. Mirzadegan, P.W. Dunten, Exploration of piperidin-4-yl-aminopyrimidines as HIV-1 reverse transcriptase inhibitors. *N*-Phenyl derivatives with broad potency against resistant mutant viruses. *Bioorg. Med. Chem. Lett.* 20 (2010) 6020-6023.
- [24] D. Li, P. Zhan, E. De Clercq, X. Liu, Strategies for the design of HIV-1 non-nucleoside reverse transcriptase inhibitors: lessons from the development of seven representative paradigms. *J. Med. Chem.* 55 (2012) 3595-3613.

- [25] Z.-Y. Wan, J. Yao, Y. Tao, T.-Q. Mao, X.-L. Wang, Y.-P. Lu, H.-F. Wang, H. Yin, Y. Wu, F.-E. Chen, E. De Clercq, D. Daelemans, C. Pannecouque, Discovery of piperidin-4-yl-aminopyrimidine derivatives as potent non-nucleoside HIV-1 reverse transcriptase inhibitors. *Eur. J. Med. Chem.* 97 (2015) 1-9.
- [26] D. Kang, Z. Fang, Z. Li, B. Huang, H. Zhang, X. Lu, H. Xu, Z. Zhou, X. Ding, D. Daelemans, E. De Clercq, C. Pannecouque, P. Zhan, X. Liu, Design, synthesis and evaluation of thiophene[3,2-d]pyrimidine derivatives as HIV-1 non-nucleoside reverse transcriptase inhibitors with significantly improved drug resistance profiles. *J. Med. Chem.* 59 (2016) 7991-8007.
- [27] T.J. Tucker, S. Saggar, J.T. Sisko, R.M. Tynebor, T.M. Williams, P.J. Felock, J.A. Flynn, M.-T. Lai, Y. Liang, G. McGaughey, M. Liu, M. Miller, G. Moyer, V. Munsh, R. Perlow-Poehneit, S. Prasad, R. Sanchez, M. Torrent, J.P. Vacca, B.L. Wan, Y. Yan, The design and synthesis of diaryl ether second generation HIV-1 non-nucleoside reverse transcriptase inhibitors (NNRTIs) with enhanced potency versus key clinical mutations. *Bioorg. Med. Chem. Lett.* 18 (2008) 2959-2966.
- [28] R. Pauwels, J. Balzarini, M. Baba, R. Snoeck, D. Schols, P. Herdewijn, J. Desmyter, C.E. De, Rapid and automated tetrazolium-based colorimetric assay for the detection of anti-HIV compounds. *J. Virol. Methods* 20 (1988) 309-321.
- [29] P. Christophe, D. Dirk, D.C. Erik, Tetrazolium-based colorimetric assay for the detection of HIV replication inhibitors: revisited 20 years later. *Nat. Protoc.* 3 (2008) 427-434.
- [30] G. Tang, D.J. Kertesz, M. Yang, X. Lin, Z. Wang, W. Li, Z. Qiu, J. Chen, J. Mei, L. Chen, T. Mirzadegan, S.F. Harris, A.G. Villasenor, J. Fretland, W.L. Fitch, J.Q. Hang, G. Heilek, K. Klumpp, Exploration of piperidine-4-yl-aminopyrimidines as HIV-1 reverse transcriptase inhibitors. N-Phenyl derivatives with broad potency against resistant mutant viruses. *Bioorg Med Chem Lett* 20 (2010) 6020-6023.
- [31] A.N. Jain, Scoring noncovalent protein-ligand interactions: a continuous differentiable function tuned to compute binding affinities. *J. Comput. Aided Mol. Des.* 10 (1996) 427-440.
- [32] A.N. Jain, Surfex: fully automatic flexible molecular docking using a molecular similarity-based search engine. *J. Med. Chem.* 46 (2003) 499-511.
- [33] L. Qian, M. Brian, S. Karl, S. Julian, Tagged fragment method for evolutionary structure-based de novo lead generation and optimization. *J. Med. Chem.* 50 (2007) 5392-5402.
- [34] J.-Z. Chen, J. Wang, X.-Q. Xie, GPCR structure-based virtual screening approach for CB2 antagonist search. *J. Chem Inf. Model.* 47 (2007) 1626-1637.
- [35] S. Raduner, A. Majewska, J.Z. Chen, X.Q. Xie, J. Hamon, B. Faller, K.H. Altmann, J. Gertsch, Alkylamides from echinacea are a new class of cannabinomimetics. *J. Biol. Chem.* 281 (2006) 14192-14206.
- [36] J. Ruppert, W. Welch, A.N. Jain, Automatic identification and representation of protein binding sites for molecular docking. *Protein Sci.* 6 (2010) 524-533.
- [37] W. Welch, J. Ruppert, A.N. Jain, Hammerhead: fast, fully automated docking of flexible ligands to protein binding sites. *Chem. Biol.* 3 (1996) 449-462.

Highlights

1. A series of indazolyl-substituted piperidin-4-yl-aminopyrimidines (IPAPYs) as HIV-1 NNRTIs were designed and synthesized.
2. The target molecules displayed moderate to excellent activities against wild-type (WT) HIV-1 with EC_{50} values ranging from 1.5 to 0.0064 μ M.
3. **5q** displayed the most excellent activities against WT HIV-1 (EC_{50} = 6.4 nM, SI = 2500).

Journal Pre-proof

Declaration of Interest Statement

This is to state that all of our co-authors approved the submission of the article titled “Indazolyl-substituted piperidin-4-yl-aminopyrimidines as HIV-1 NNRTIs: design, synthesis and biological activities” to *Eur. J. Med. Chem.* We declare that we have no conflict of interest.

Ting Xiao, Jia-Fan Tang, Ge Meng, Christophe Pannecouque, Yuan-Yuan Zhu,
Gen-Yan Liu, Zhi-Qiang Xu, Feng-Shou Wu, Shuang-Xi Gu*, Fen-Er Chen*